Low-power wireless microsystems for use with thermoelectric scavenging systems

J. P. Carmo, R. P. Rocha, A. F. Silva, P. M. Mendes, L. M. Goncalves, J. H. Correia
University of Minho, Dept. Industrial Electronics
Campus Azurem, 4800-058 Guimaraes, PORTUGAL, jcarmo@dei.uminho.pt

Abstract - **RF microsystems constituted by low-power/low-voltage devices for use in wireless sensors networks are presented in this paper. The major emphasis is given to the fabrication of RF transceivers for integration in such a microsystems. Features concerning the low-power and low-voltage operations are discussed, at the same time the presentation of RF transceivers for operation in the of 2.4 GHz and 5.7 GHz ISM bands is made. The grown interest to implement the paradigm of used independent operation, management and maintenance in wireless sensors networks, pushed the requirements in WSN nodes to present even more low-power consumptions. This is of major importance, specially in wireless microsystems to be supplied by thermoelectric energy scavenging systems.**

I. INTRODUCTION

The successful penetration in the market, of devices comprising the use of wireless microsystems, is conditioned by its usefulness and the final price. By reducing the complexity, size and consumption of such systems, the former goals can be achieved. Directly connected to the size and complexity, the microsystems must contain at least a radio-frequency (RF) transceiver, the electronics of processing and control, and the sensors to gather signals. Thus, it must be possible to make microsystems with low-power consumptions and low-voltage supplies, in order to be possible the use batteries with small dimensions, by long time periods. The number of sensors and places to be monitored can be large, thus in order to delivery the acquired data in a reliable form, it must be possible to use the RF transceiver as a node in a wireless sensors network. To optimize the power consumption, RF transceivers must predicts the use of control signals, which make possible to enable and disable the transceiver subsystems. These signals allows to switch off the receiver when a RF signal is being transmitted, to switch off the transmitter when a RF signal is being received, and the transceiver to enter to sleep when RF signals are neither being transmitted nor being received. As is of common knowledge, the CMOS technology has reached its maturity. Therefore, designers used it for developing RF circuits. The advantages of CMOS technology are higher integration, low-power consumption, low-voltage supply and low-cost compared with bipolar technology. Using CMOS processes with low channel's length is very important for high-frequency devices. This paper presents several wireless microsystems for use in wireless sensors networks and for a wide variety of frequencies. In this sequence, and as will be seen further, this was one of the main reasons that were behind the chose of a 0.18 μm CMOS process to design, optimize and fabricate, radio-frequency (RF) transceivers for the operation in frequencies such as the 2.4 GHz and 5.7 GHz. The need to have low-power consumption stand-alone devices, is due to the necessity to supply it from thermoelectric microdevices, in order to eliminate the need of maintenance (charging or replacement of batteries). Moreover, the available thermoelectric microdevices that make use of conventional materials (rather than super-lattice materials) have low figure-of-merits (the supplied electrical power versus the temperature gradient) [1].

II. SYSTEM REQUIREMENTS

In wireless communications, the antenna is one of the most critical subsystem, thus, in order to not compromise the desired miniaturization, the antenna must be small enough to comply with size constraints of the microsystems. The investigation of new frequency bands [2] and new geometries [3] will make possible to have smaller antennas to integrate in wireless microsystems [4,5]. This makes the chose of the most suitable frequency, one of the more decisive aspects in the design of RF transceivers. Normally, the desired range, baud-rate and power consumptions are key-aspects in the design to take in account, when the frequency of operation is to be selected. At a start-up point, the range limits the maximum usable frequency, because the loss suffered by the radiowaves in the free-space increases with the distance. However, to keep or even increase the useful life of the batteries, such a variation in the transmitted power is not possible to do. Moreover, in the case of applications requiring higher baud-rates, the transmitted bandwidth must also be higher, in order to support these applications. However, the frequency can't be arbitrarily increased, because this have implications in the power consumptions, e.g., at high frequencies, the transistors must switch faster, thus the energy dissipation will be bigger. Fig. 1 shows the available frequency bands for the different technologies used in wireless communications. The most suitable frequencies are those belonged to the so called ISM band (Industrial, Scientific and Medical), due to its unregulated usage, e.g., these frequencies are not subjected to standardization and can be freely used, since the emitted power are maintained below the maximum levels imposed by the legislation. Such a flexibility leaded to the rising and spreading of interesting applications.

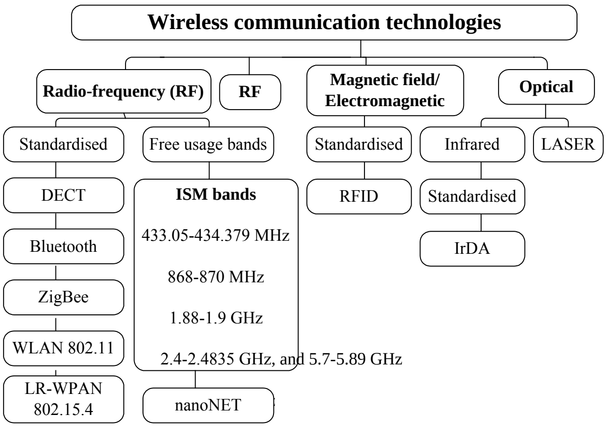

Fig. 1: Available frequency bands and respective applications.

III. WIRELESS MICROSYSTEMS

Fig. 2 shows the block diagram and the respective interface for monitoring the body movements of individuals. This interface connects to a set of accelerometers with three axis, which are used to measure the relative position of members to the thorax. This was the first attempt to have a real wireless interface for data acquisition and transmission using the wireless sensors network paradigm. This interface uses an analog multiplexer followed by an analog-to-digital converter (ADC) to acquire and process the signals. All of the analog electronics of control and processing is managed using the control logic of the interface. A third party RF module the uses a 2.4 GHz wireless link to exchange data.

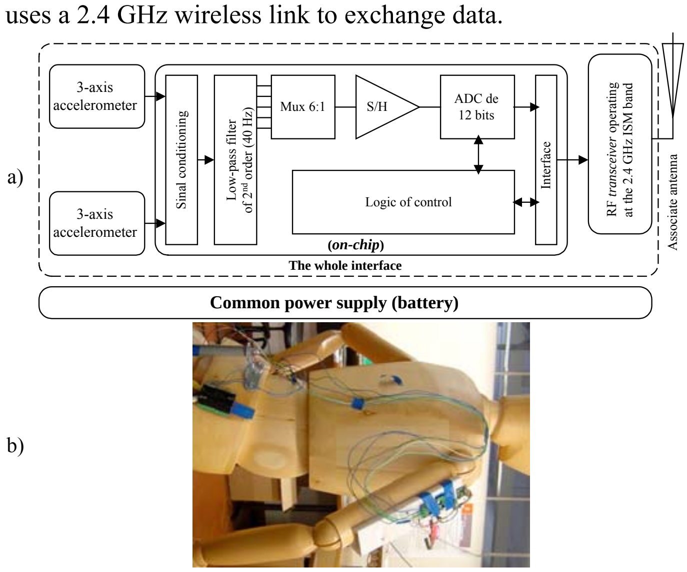

Fig. 2: a) The block diagram of a wireless interface for the 2.4 GHz, and b) an interface mounted in the arm of a test-dummy (the photography is 90º rotated).

Higher frequencies such as those in the range 5.7-5.89 GHz makes possible to have antennas sufficiently small, in order to fabricate microsystems, containing the wireless interface and antenna. Moreover, these kind of solutions helps to reduce the problems related to impedance mismatches, while at the same time, it increases the systematization of the manufacturing processes and delivers microsystems with an even reduced price [6]. Fig. 3(a) shows a microsystem, where it can be seen the RF transceiver mounted together with a chip-size antenna of planar type, which were optimized and fabricated for the operation in the 5.7 GHz ISM band and measures 7.6×7.7mm [5]. The microdevice shown in Figure 3(b), is the RF transceiver used for the transmission at 5.7 GHz. This RF transceiver uses the ASK modulation to transmit the data. As stated before, the chose of the best suitable technology, felt in a 0.18 µm CMOS process, because it allows to trade the high-frequency capability of minimum-length transistors with lower current consumption by biasing the devices at lower current densities, even for devices working at RF. This process provides a poly and six metal layers, the use of integrated spiral inductors (with a quality factor of ten), high-resistor values (a special layer is available) and with a low power-supply. The transceiver has a Low-Noise Amplifier (LNA) that provides a 50 Ω input impedance, the amplified RF signal is directly converted to the baseband with a single balanced active MOS mixer. The internal oscillator is a Phase-Locked Loop (PLL) working at 5.7 GHz. The transceiver is able to operate at the [5.4200–5.8265 GHz] frequency range. This is done by changing the frequency division ratio in the feedback path of the PLL. The PLL has four digital inputs for the division ratio programming. The output frequency is $f_{out}=f_{ref}\times 2\times(200+D)$, where D is the decimal representation of the division ratio. The used reference frequency was f_{ref}=13.56 MHz. In high frequency PLLs, the high power consumption is mainly due to the first stages of the frequency divider that often dissipates half of the total power. At frequencies in the range [5.420-5.827 GHz], the measurements show for the LNA a gain in the range [9.597-9.807 dB], a NF in the range [0.775-0.841 dB] and a stabilization factor K of 1.209, making the LNA unconditionally stable (K>1). Measurements show for the LNA, a power consumption of 9.65 mW. The power consumptions are about of 9.51 mW for the mixers, and 4.14 mW for the PLL.

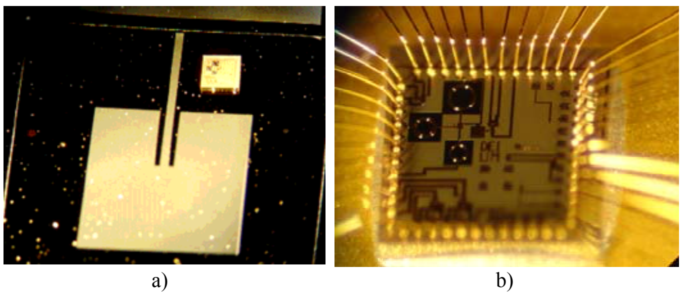

Fig. 3: a) Chip-size antenna for operation at 5.7 GHz assembled with a RF transceiver, and b) a magnified photograph of the same RF transceiver.

In wireless sensors networks, the continuous working time of sensorial nodes are limited by its average power consumption [7]. Thus, in the majority of the applications, the contributions of the electronics in a node has a low contribution in the total power consumption of this node. In fact, the fact of the available technologies be more and more low-power, this don't relief the fact the transceiver be the bloc with the bigger power consumption [8]. The co-definition of new architectures and algorithms is a topic of even more concern, in order to quantify in advance the exact implication of the RF system in the total power consumption [9]. To conclude, without proper design, communication will increase network power consumption significantly because listening and emitting are power-intensive activities [10]. Thus, in order to optimize the power consumption, it was designed a RF transceiver for the operation in the 2.4 GHz ISM band (known as RF CMOS transceiver) [11]. It was used the same 0.18 µm CMOS process used in the fabrication of the 5.7 GHz RF transceiver, which were presented previously. Moreover, in order to optimize power management, the RF transceiver design predicts the use of control signals. With these control signals it is possible to enable and disable all the subsystems of the transceiver. These signals allows, e.g., to switch off the receiver when a RF signal is being transmitted, to switch off the transmitter when a RF signal is being received, and allows the transceiver to enter to sleep when RF signals are neither being transmitted, nor being received. An important feature that this RF CMOS transceiver must allow, is the possibility to be integrated together in the same microsystem with sensors and the remain electronics of processing and control, in order to reduce the number of supply-points. This makes more practical and easy to supply all the subsystems, since it needs to attach a single battery. Fig. 4 shows the schematics of the RF CMOS transceiver, which consists of a receiver, a transmitter, an antenna-switch and a Phase-locked Loop (PLL) as a frequency synthesizer. The receiver adopts a direct demodulation, by means of envelope detection. The transmitter is constituted by a chain of subsystems, which the first of all is a modulator circuit, where a preliminary version of a digital ASK signal is generated to be combined with the bitstream to be transmitted at the frequency of 2.4 GHz. Then, this signal enters in an external filter, followed by a switched Power Amplifier (PA), whose output is the modulated ASK signal at the input of the antenna. The 2.4 GHz carrier is locally generated by the PLL.

The power budget of the RF link must be made, in order to have in any noise condition and with the maximum baud-rate of 250 kbps, a bit error probability (BEP) less that 10^{-6} (BEP=$P_e \leq 10^{-6}$). This target quality of service (QoS) is for a maximum transmitted power of 0 dBm (1 mW) with Amplitude Shift Keying (ASK) modulation. Using an antenna with an output impedance of 50 Ω (at the frequency of 2.4 GHz) and a Spectrum Analyzer, model *Agilent E4404-B*, it was made several measurements of the environment noise. It was observed that the noise power never crossed above N=-104 dB. The previous known of noise levels and the QoS of the system are mandatory, in order to know the minimum sensitivity of the receiver. From the BEP of ASK with envelope detection (also known as non-coherent ASK systems) [12], given by $P_e = ½e^{-\gamma/2}$, $\gamma \gg 1$, where γ is the signal-to-noise ratio (SNR) at the receiver and to have $P_e \leq 10^{-6}$, it is necessary a minimum SNR in the receiver site of $\gamma \geq 26$ (γ=14 dB). This imposes a minimum signal power, S_{min}, in the receiver such that $\gamma = S_{min} - N \geq 14$ dB. Then, the sensitivity of the receiver must be at least $S_{min}=14+N=-90$ dB (-60 dBm). Starting with the transmitted power of P_t=0 dBm and applying the Friis formula: $L_f(d_m)=20\log_{10}[75/(\pi d_m \cdot f_{MHz})]$ [dB], where d_m is the distance [m] and f_{MHz} is the frequency [MHz], the SNR for a ten meters range is such that $\gamma_0 = P_t - L_f(d=10\text{m}) - N \cong +13.96$ dB. This SNR is very close the required +14 dB, thus it is not necessary to modify the specifications of the transceiver. The receiver's front-end is a chain composed of a Low-Noise Amplifier (LNA), a post-amplifier, and an envelope detector. The post-amplifier provides additional gain to the RF signal coming from the LNA and the envelope detector senses the presence of the 2.4 GHz carrier. Then, after the envelope detection, the resulted signal is injected in the output buffer, in order to transform it in a perfect NRZ rail-to-rail signal.

b)

b)

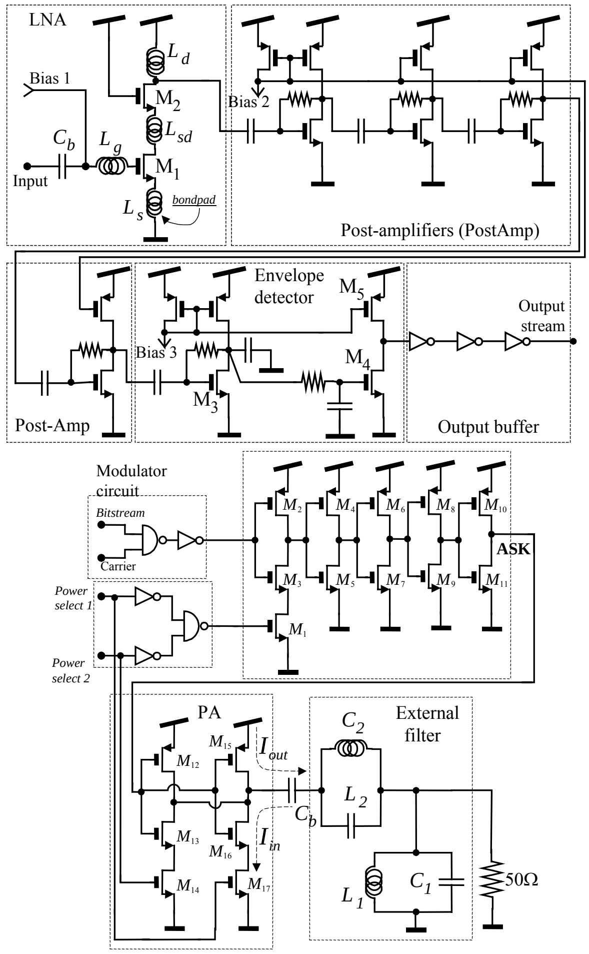

Fig. 4: The schematics a) of the receiver, and b) of the transmitter.

The PA allows to select the transmitted power, e.g., two control lines allows to select the transmitted power and to switch off the PA. Furthermore, an internal antenna-switch makes this transceiver a true complete system-on-a-chip (SOC). The antenna-switch connects the antenna to one of the receiver or transmitter path, that are connected to the receiving and transmitting ports, respectively. The isolation between non-connected ports must be high. In order to have a power efficient transceiver without degrading its sensitivity, the losses in the switch must be low.

For analog blocks, the Fig. 5(a) shows the principle used to switch on and off. The transistors M_{1x} are normally in the cut-off state due to theirs gate-source voltages be zero. However, when a voltage, $V_{control}$ of 1.8 V is applied, they start to conduct; then the current sources constituted by the transistors M_{2a} e M_4 are activated. M_4 behaves like a resistor, thus making the transistors M_{2b}, M_{2c} and further (if more were available) behaving like current sources, e.g., they start to inject current in the branches *Bias* 1 and *Bias* 2. In a same way, the current sources constituted by the transistors M_{5a} e M_3, are also activated, which makes the transistors M_{5b}, M_{5c} and further, behaving like sinks. These sinks absorbs the currents which travels from the branches *Bias* 3 and *Bias* 4. Fig. 5(b) shows the principle to control digital blocks, and it can be seen the addition of the transistor M_3 to the inverter constituted by M_1 and M_2. Normally, the M_3 is also in the cut-off state, because as in the previous case, its gate-source voltage is also zero, thus the power consumption of the inverter will be zero. Digital drivers with high-impedance outputs applied in digital buses use this same principle, when outputs with high impedances are desired. Fig. 6 shows a photograph of the first prototype of a low-power/low-voltage RF CMOS transceiver, which occupies an area of 1.5×1.5 mm^2.

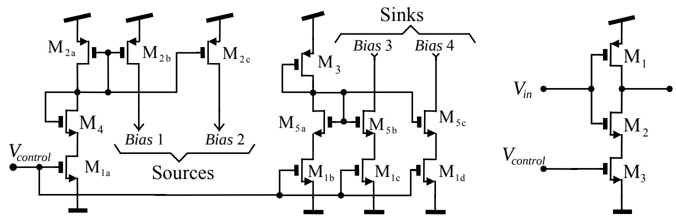

a) b)

Fig. 5: a) Principle used to enable and disable analog blocks; and b) principle used to enable and disable digital blocks.

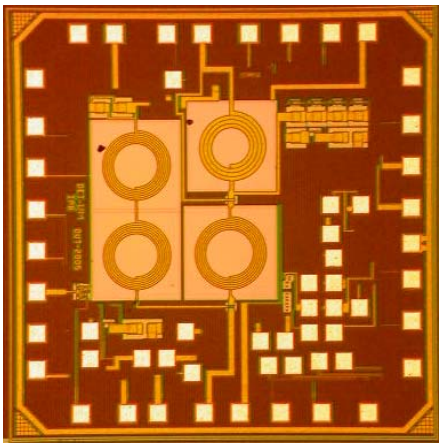

Fig. 6: A die photograph of the RF CMOS transceiver.

The experimental tests made to the RF CMOS transceiver, shown a total power consumption of 6.3 mW for the receiver (4 mW for the LNA, and 2.3 mW for the envelope detector and for the post-amplifier), and 11.2 mW for the transmitter. The transmitter delivers a maximum output power of 1.28 mW (very close to the specified 0 dBm) with a power consumption of 11.2 mW. When enabled, the power at the output of the PA, can be selected from the following values: 0.22 mW, 1.01 mW and 1.21 mW. It was observed for the LNA, a S_{21} of 19.2 dB, a noise figure (NF) of 3 dB, a 1 dB compression point (IP1) of -9 dBm, and a third order intercept point (IP3) of -5.4 dBm. The LNA has also a stabilization factor of K=1.8 (grater than the unity), that makes this amplifier unconditionally stable.

The interest in the development of low-power/low-voltage wireless microsystems is justified by the fact that energy scavengers are currently emerging for a number of applications from automotive to medicine. Micro energy scavengers are small devices which harvest ambient energy and convert it into electricity. It exists two types of energy scavenging systems: macro energy scavengers, typically in the cm^3 range, and micro energy scavengers, typically in the mm^3 range and manufactured using micromachining techniques. Micro energy scavengers are still in the R&D phase. Direct thermal-to-electric energy conversion without moving mechanical parts is attractive for a wide range of applications because it provides compact and distributed power, quiet operation, and is usually environmentally friendly. Thus, worldwide efforts are undertaken to expand the technology of thermoelectric devices into the field of micro-systems technologies (MEMS). Previsions made by the specialists of the microsystems area, shows that the most expected growth of these devices, will be with medical applications. An emerging technology for ultra-low power communication platforms triggered renewed interest in power sources for wireless-sensor, in special wireless-wearable-sensors, with power consumption nodes of few mW. Today, almost all of these platforms are designed to run on batteries which not only have a very limited lifetime, but are also in many areas a cost-prohibitive solution. An attractive alternative is powering the sensors with energy harvested from the environment. Thus, it is growing, the interest of solutions for energy microgeneration through energy harvesting by taking advantage of temperature differences. This temperature difference can be converted into electrical energy using the Seebeck principle. Since many of wireless sensors are powered in a peak basis (e.g., the transmission of data needs much more current than standby or receiving mode) and the temperature gradient could not always be present, the energy is stored in a rechargeable thin-film battery of the Li-ion type (integrated in the system). Ultra-low power electronics performs DC-DC rectification with a variable conversion factor and recharge the battery on optimal conditions. Since a small volume is required, integration into an IC is desirable. A single-chip regulated thermoelectric power source is the final goal to be achieved [14]. Previous works [15,16] has demonstrated the maximum amount of thermal energy that can be removed from human-body in a wearable thermal-generator without compromising the comfort, and maximizing the thermoelectric conversion.

Future investigations, must prove if the operation from low temperature gradients (a minimum temperature difference of 3 ºC between ambient and target thermo-source must provide an IC-compatible voltage) and the power of 2 mW/cm^2 are possible to be obtained. The fabrication of macro-scale thermoelectric devices is based on standard technologies for decades. Bismuth and antimony tellurides was be used as thermoelectric materials since these materials have the highest performance figure-of-merit (*ZT*) at room temperature [17]. The co-deposition method was used to fabricate these thermoelectric thin films. A very stable evaporation rate of each element (Bi/Te and Sb/Te for the bismuth telluride and antimony telluride, respectively) allows the deposition of polycrystalline n-type and p-type materials, when the substrate is heated in the range 200-300 ºC (Fig. 7 shows SEM images of both thin-films). As shown in Fig. 8, the design of a thermoelectric microdevice, with vertical microcolumns, connected in series by metal contact areas, requires the application of microsystem technologies [18]. Reactive ion etching, lift-of and wet-etching techniques were tested to create the vertical columns. A thin (50 nm) layer of nickel (deposited by e-beam) interfaces between the thermoelectric material and the metal contact areas (1 µm of aluminum), preventing the diffusion of the metal from the contacts into the thermoelectric film. The contact resistance plays a major role in the performance of the device, and a value smaller then 1×10^{-6} $\Omega.cm^2$ was achieved. A silicon substrate was used for integration with microelectronics, while at same time providing good thermal contact with heat source and sink. The fabricated battery, as well as, all the electronic circuitry to receive the energy and to recharge the thin-film integrated Li-ion battery (open circuit voltages between 1.5 V and 4.2 V, maximum current of few mA/cm^2 with a charge-storage capacity around 100 $\mu Ah/cm^2$), was placed on the bottom side of the generator. Thin-film solid-state batteries show a very high life cycle and are intrinsically safe [19].

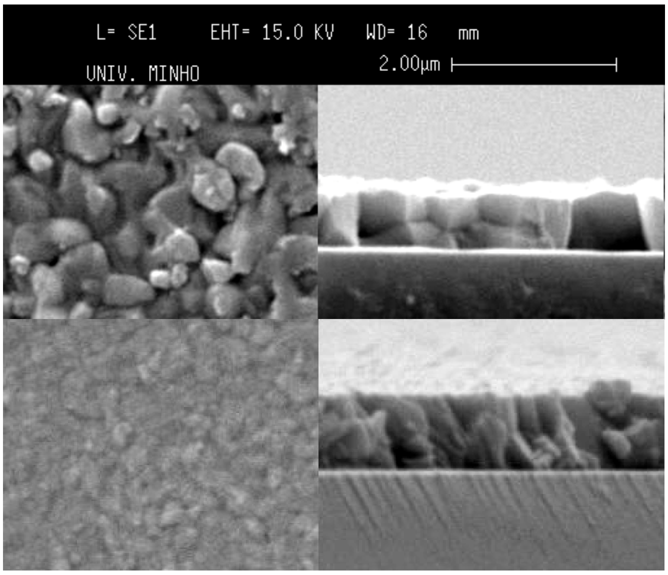

Fig. 7: SEM top view (left) and cross-sectional (right) images of Bi_2Te_3 (top) Sb_2Te_3 (bottom) thin-films.

Fig. 9 shows a cross-section of the solid-state lithium battery, in whose fabrication was employed the DC reactive sputtering technique. The battery uses tin dioxide (SnO_2), lithium phosphorus oxynitride (lipon) and lithium cobaltate ($LiCoO_2$) materials respectively in the anode, electrolyte and cathode. SnO_2 have a maximum theoretical charge-storage capacity of 781 mAh/g and $LiCoO_2$ anode have a specific capacity of 140 mAh/g, with voltages between 3 V and 4.2 V. Lipon is sputtered from lithium phosphorus tetraoxide (Li_3PO_4) target in N_2/Ar plasma. The lipon electrolyte has exceptional electrochemical stability and good Li^+ ion conductivity (2×10^{-6} S/cm). The self-discharge of the battery is ensured with the high electronic resistivity of the Lipon (10^{14} Ωcm). Fig. 10 shows a SEM top view and cross-sectional images of the $LiCoO_2$ and SnO_2 thin-films.

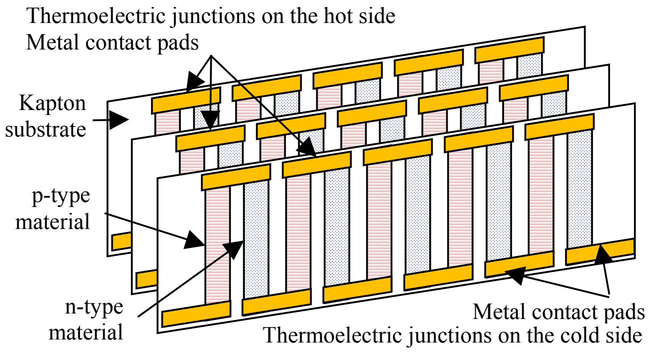

Fig. 8: Artwork of the proposed device.

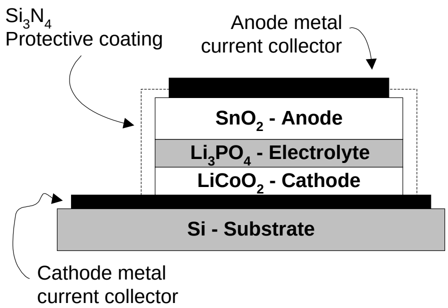

Fig. 9: Cross-section of the thin-film rechargeable battery.

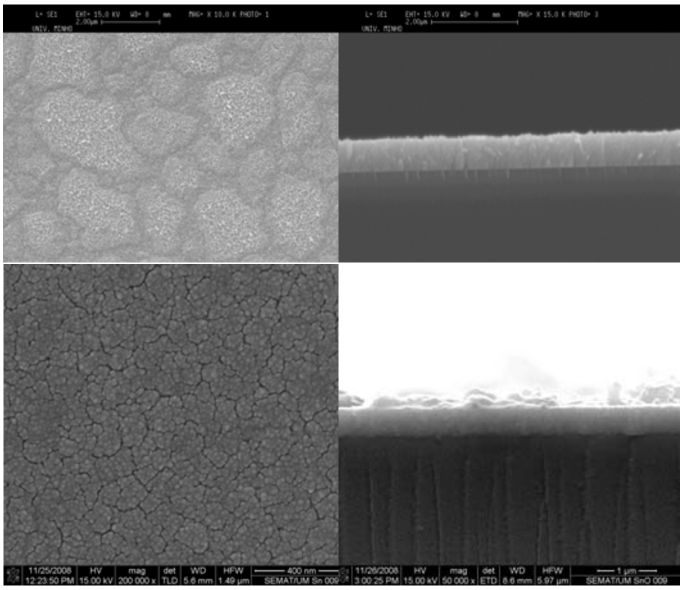

Fig 10: SEM top view (left) and cross-sectional (right) images of $LiCoO_2$ (top) SnO_2 (bottom) thin-films.

As the final goal of thermoelectric scavenging energy systems are to supply the wireless acquisition modules in wireless sensors networks, these must present low-power consumptions in order to match with the power sources, as a way to put these same modules to works without human intervention, e.g., either to switch the battery or to recharge it.

IV. *HOT*-FEATURES CONCERNING ESD PROTECTIONS

Normally, during the chip design, it is necessary to prevent two effects that can arise: the first is the latch-up. This effect can change the behavior of the circuit and destroy it [20]. Another effect is the Electrostatic Discharge (ESD), which can cause its destruction [21]. During the design of the transceiver in Fig. 6, two levels of protections were considered: the protection of the circuits, that connects to the bondingpads, and another to avoid the destruction of the internal circuits, from supply-rails discharges. This protection is achieved with power clamps, e.g., a transistor of N-type with its gate connected to the ground. For this transceiver, the capacitance of ESD protection diodes is 1.57 pF, thus the LNA is not anymore matched with the antenna. This increases the return loss at the input, making the range smaller, for the same power transmission. Calculations shown a decrease in the range, from 10 meters to 5.5 meters. The solution is the use of external elements to have again, a perfect match between the LNA and antenna. Solutions improve the behavior of the circuit. The first uses a classical matching network, which consists on a series inductance, L_s=1.5nH and a parallel capacitor, C_p=3pF; while the second uses a series-stub (with characteristic impedance of 40 Ω and an electrical length of 30º) and a open-circuited parallel-stub (with characteristic impedance of 55 Ω and an electrical length of 69º). Fig. 11 shows four situations for the reflection coefficient (k_R) at the input of the LNA. In two both matching situations, the reflections decreases to acceptable values.

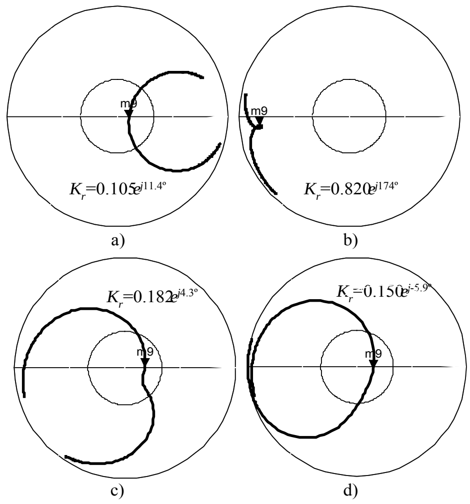

Fig. 11: Reflection coefficient (k_R) a) ideally, without the effect of the ESD protections; b) with the effect of the ESD protections; c) with compensation network formed by lumped elements, and d) with a compensation network formed by transmission lines.

The power-clamp, is a transistor of N-type with the gate and source connected to the ground and with its drain connected to the V_{dd} (1.8 V) supply-rail, thus this transistor is normally in the cut-off state [22], and uses a serial resistance to limit the discharge currents to prevent the destruction of the microdevice. The implantation of a supplementary layer in the zone of drain, helps to make the ESD protections more effective and themselves more robust to discharge currents. The widths of the N-type transistors must be as high as possible, to have a better flow of discharge currents [23]. This power-clamp is a parallel of four (#4) N-type transistors, whose individual ratios are W/L = 12.5/0.36 [μm/μm]. It was analyzed the behavior of the power-clamp, when subjected to a ESD voltage of 4 kV. The obtained results revealed to be promising, because it was obtained a maximum discharge current of 32 mA and a voltage between the drain and the source of the transistor below 35.4 V. This makes the dissipated power to be only 1.13 W. Moreover, the use of transistors with ratios W/L = 12.5/0.36 [μm/μm], decreases the parasitic capacitance between the drain and the source, with the consequence to have less interferences with the radio-frequency signals.

V. FUTURE TRENDS

The future of RF microsystems pass with the use of MEMS (Micro Electro Mechanical Systems) based components [24]. An example of such a component can be the generator of the reference frequency used in the PLL. Crystal-based piezoelectric oscillators normally require a huge areas, compared with those used by the associated electronics (when they exist, the inductances and capacitors are not included in this set), thus an additional space must be provided in the PCB (Printed Circuit Board) with the inevitable consequence of an increase in the total production cost. Moreover, the accuracy and the stability of the produced frequency by these oscillators are temperature dependant and the error will be multiplied by the PLL, e.g., if the actual reference frequency is $f_{ref2}=f_{ref}\times(1\pm\Delta f)$, the carrier frequency at the output of the PLL will be $f_{out2} = N.f_{ref2} = N.f_{ref} \pm N.f_{ref}.\Delta f = f_{out} \pm \Delta f_{out}$, where N is the division ratio of a PLL, f_{ref} [Hz] is the error-free reference frequency of a PLL, $\pm\Delta f$ [Hz] is the drift (above or below) in the reference frequency, f_{out} [Hz] is the error-free carrier frequency. A special concern must be taken in account, specially for high division ratios, N, and high reference frequencies, f_{ref} [Hz], in the PLL, because the overall drift (or propagated error) in the frequency at the output of the PLL, $\Delta f_{out} = N.f_{ref}.\Delta f$ [Hz], can be critical. Beyond the advantage to have a small area occupancy, MEMS resonators allows to make an accurate trimming in the frequency of oscillation. Moreover, the simple matter of fact this adjustment could be made in the electrical domain, constitutes an inexorable advantage over the Crystal oscillators [25].

ACKNOWLEDGEMENTS

This work was supported by Foundation for Science and Technology FCT/PTDC/EEA-ENE/66855/2006 project.

REFERENCES

[1] W. Wang, *et al*, “A new type of low power thermoelectric micro-generator fabricated by nanowire array thermoelectric material”, Microelectronic Engineering, Vol. 77, pp. 223-229, 2005.

[2] N. Celik, *et al*, "Implementation and experimental validation of a smart antenna system operating at 60 GHz band", IEEE Transactions on

Antennas and Propagation, Vol. 56, No. 9, pp. 2790-2800, September 2008.
[3] P. Mendes, *et al*, “Integrated chip-size antennas for wireless microsystems: Fabrication and design considerations”, Journal Sensors and Actuators A, Vol. 125, pp. 217-222, January 2006.
[4] F. Touati, M. Pons, “On-chip integration of dipole antenna and VCO using standard BiCMOS technology for 10 GHz applications”, in Proc. 29th ESSCIRC, pp. 493-496, Estoril, Portugal, September 2003.
[5] J. Carmo, *et al*, “5.7 GHz on-chip antenna/RF CMOS transceiver for wireless sensors", Journal of Sensors and Actuators - A, Vol. 132/1, pp. 47-51, ScienceDirect, November 2006.
[6] E. Callaway Jr., Wireless sensor networks, Architectures and protocols, Chapter 3: The physical layer, CRC Press, 2004.
[7] E. Mackensen, *et al*, “Enhancing the lifetime of autonomous microsystems in wireless sensor actuator networks (WSANs)”, in Proc. of the XIX Eurosensors, Barcelona, Spain, 2005.
[8] J. Gutierrez, *et al*, "IEEE 802.15.4: Develping standards for low-power low-cost wireless personal area networks", IEEE Network, pp. 2-9, September 2001.
[9] C. Enz, *et al*, “Ultra low-power radio design for wireless sensor networks”, in Proc. IEEE International Workshop on Radio-Frequency Integration Technology: Integrated Circuits for Wideband Communication and Wireless Sensor Networks, December 2005.
[10] C. Enz, *et al*, “WiseNET: An ultralow-power wireless sensor network solution”, IEEE Computer, Vol. 37, No. 8, pp. 62-70, August 2004.
[11] J. P. Carmo, *et al*, "A 2.4-GHz Low-Power/Low-Voltage Wireless Plug-and-Play Module for EEG Applications", IEEE Sensors Journal, Vol. 7, No. 11, pp. 1524-1531, November 2007.
[12] B. Carlson, *et al*, Communication systems: An introduction to signals and noise in electrical communications, 4th edition, McGraw-Hill, 2002.
[13] J. Parsons, The mobile radio propagation channel, Wiley, 2000.
[14] L. M. Goncalves, *et al*, "A human-body thermoelectric energy scavenging microsystem", in Proc. of MME 2008, Aachen, Germany, pp. 49-52, September 2008.
[15] V. Leonov *et al*, “Thermoelectric MEMS Generator As A Power Supply For A Body Area Network”, in Transducers ’05, pp.291-294,2005.
[16] R. J. M. Vullers, *et al*,, “Energy Scavengers For Wireless Intelligent Microsystems”, OnBoard Technology 06/2006, pp. 34-37.
[17] L. M. Gonçalves, *et al*, "Thermoelectric properties of Bi2Te3/Sb2Te3 thin films", Materials Science Forum, Vols. 514-516, pp. 156-160, 2006.
[18] L. M. Gonçalves, *et al*, "Fabrication of flexible thermoelectric microcoolers using planar thin-film thecnologies", Journal of Micromechanics and Microengineering, Vol. 17, pp. 168-173, 2007.
[19] J. Bates, *et al*, "Thin-film lithium and lithium-ion batteries", Solid State Ionics, Vol. 135, pp. 33-45, 2000.
[20] M. Ker, W. Lo, “Methodology on extraction compact layout rules for latch-up prevention in deep-submicron bulk CMOS technology”, IEEE Transactions on Semiconductor Manufacturing, Vol. 16, No. 12, pp. 319-334, May 2003.
[21] J. Vinson, J. Liou, “Electrostatic discharge in semiconductor devices: An overview”, Proceedings of the IEEE, Vol. 86, No. 2, pp. 399-418, February 1998.
[22] M. Ker, *et al*, “ESD implantation for sub-quarter-micron CMOS technology to enhance ESD robustness”, IEEE Transactions on Electron Devices, Vol. 50, Nr. 10, pp. 2126-2134, October 2003.
[23] UMC 0.18μm ESD design rules, UMC SPEC No. G-1B-029, Ver 8.0, Phase 1, April 2005.
[24] C. Nguyen, *et al*, "Micromachined devices for wireless communications", Proceedings of IEEE, Vol. 86, No. 8, pp. 1756-1768, August 1998.
[25] J. Yao, "RF MEMS from a device perspective", Journal Micromechanical Microengineering, Vol. 10, pp. 9-38, 2000.